Chapter 16

Sample-to-Answer Microfluidic Nucleic Acid Testing (NAT) on Lab-on-a-Disc for Malaria Detection at Point of Need

Gihoon Choi and Weihua Guan

Abstract

One of the grand challenges for field-deployable NATs is related to the front end of the assays—nucleic acid extraction from raw samples. The ideal nucleic acid sample preparation should be simple, scalable, and easy-to-operate. In this chapter, we present a lab-on-a-disc NAT device for sample-to-answer malaria diagnosis. The parasite DNA sample preparation and subsequent real-time LAMP detection are seamlessly integrated on a disposable single microfluidic compact disc, driven by energy-efficient, non–centrifuge-based magnetic field interactions. Each disc contains four parallel testing units, which could be configured either as four identical tests or as four species-specific tests. When configured as species-specific tests, it could identify two of the most life-threatening malaria species (*P. falciparum* and *P. vivax*). The reagent disc with a 4-plex analyzer (discussed in Chapter 1) is capable of processing four samples simultaneously with 40 min turnaround time. It achieves a detection limit of ~0.5 parasites/μl for whole blood, sufficient for detecting asymptomatic parasite carriers. The assay is performed with an automated device described in Chapter 14. The combination of sensitivity, specificity, cost, and scalable sample preparation suggests the real-time fluorescence LAMP device could be particularly useful for malaria screening in field settings.

Key words Point-of-care, Microfluidic, Nucleic acid testing, Malaria

1 Introduction

Malaria is a mosquito-borne disease caused by *Plasmodium* parasites, predominately in resource-limiting areas of low- and middle-income countries. Among five parasite species, *P. falciparum (Pf)* and *P. vivax (Pv)* pose the greatest threat to the human. *Pf* is the most prevalent malaria parasite on the African continent. *Pv* is the dominant malaria parasite in most countries outside of sub-Saharan Africa. Increased malaria control efforts have resulted in a dramatic reduction in global malaria incidence over the past decade. The World Health Organization (WHO) thus endorsed the ambitious goal of achieving worldwide malaria elimination and eradication. A change in focus from malaria control to elimination requires the identification and treatment of both symptomatic and

Miguel R. Ossandon et al. (eds.), *Biomedical Engineering Technologies: Volume 1*, Methods in Molecular Biology, vol. 2393, https://doi.org/10.1007/978-1-0716-1803-5_16,

asymptomatic carriers to reduce the parasite reservoir and interrupt malaria transmission. As a result, the effectiveness of elimination strategies highly depends on low-cost access to sensitive and specific malaria screening tests [1]. Current screening test methods rely almost exclusively on microscopy (thin and thick blood smears) and immunological rapid diagnostic tests (RDTs, detecting antigens in human blood). While they perform sufficiently well in high transmission regions for diagnosing people with symptomatic malaria, both methods could miss a significant portion of asymptomatic parasite carriers in low-transmission areas due to the detection limit of ~100 parasites/μl [2, 3]. During the course of malaria elimination, the proportion of low-density and asymptomatic infections increases, thus rapid and highly sensitive point-of-care field test is increasingly needed to identify all infected individuals for treatment.

Lower parasite density can be identified by nucleic acid tests (NATs), often by PCR, which has an excellent detection limit of <1 parasite/μl depending on the assay type [4–6]. However, PCR-based assays are poorly suited to perform in field settings as they require specialized equipment for sample preparation and skilled personnel [7]. Alternative NATs, such as loop-mediated isothermal amplification (LAMP) assays [8–17], recombinase polymerase amplification (RPA) assays [18, 19], as well as helicase dependent amplification (HAD) assays [20], have shown high analytical sensitivity and great potential for field deployment by integrating with microfluidic [21] and paper-based devices [22]. Among isothermal methods, LAMP is the most studied assay for malaria detection and holds great promise for commercialization. For instance, the illumigene malaria LAMP assays could reliably and sensitively detect *Plasmodium* by combining a manual blood sample preparation step with an incubator reader [23]. Despite great effort and progress toward field deployment of malaria NATs assays, highly integrated DNA sample preparation from raw peripheral blood for molecular assays remains a bottleneck [24, 25]. For example, current nucleic acid sample preparation is often limited at point-of-care settings due to lengthy or error-prone manual processes such as gravity-driven filtration [23] and centrifugation [26]. The ideal sample preparation should be simple, scalable, and easy-to-operate.

To bring the NATs to the field, the test assay with a streamlined sample process has been incorporated with various microfluidic-based lab-on-chip (LOC) technologies. The existing microfluidic LOC devices for NATs can be categorized based on the fluid driving mechanisms (e.g., pump-based [27], paper-based [27, 28], and centrifugal devices [29, 30]). While the pump-based approach is intuitive for precise fluid control, the benchtop syringe pump, multiple tubings, and complex valving make the system bulky and difficult to be integrated for POC application

[31]. The low-cost paper-based approach uses capillary action to move the liquid on a paper substrate; thus, reagents can be delivered sequentially without the pump and complex tubings. For example, Phillips et al. developed a microfluidic rapid and autonomous analytical device (MicroRAAD) for the RT-LAMP HIV-1 test. The device used paper membranes' wicking ability and porous structure for sequential sample process from viral particle isolation to amplification in automated fashion [28]. However, lacking adequate sensitivity and quantitative ability are challenges to be addressed [32]. Prior works on lab-on-a-disc platforms for NATs exclusively utilized centrifugal forces to drive liquid to the desired location in the microfluidic disc [29, 30]. While it works great for various diagnostic applications, the centrifugal forces are energy-hungry.

The demand for microfluidic chip fabrication technique has been increased due to the growing need for lab-on-a-chip devices in medicine and healthcare. Poly(methyl methacrylate) (PMMA) is a polymer, which is widely used for microfluidic chip fabrication due to its rigid mechanical property, optical transparency, low-cost, and rapid prototyping. Precise micromachining of PMMA is available using laser drilling or micromilling techniques. Among various lamination methodologies (e.g., thermal bonding and adhesive film), the solvent-based lamination technique showed excellent PMMA–PMMA bonding strength without requiring thermal pressing, which often causes deformation in microfluidic channel dimensions. Besides, the surface property of PMMA can be engineering by laser irradiation [33]. More specifically, PMMA becomes more hydrophilic when it is exposed to the high-power laser during the laser cutting process. Such property allows various liquid manipulation techniques such as structural-pinning effect-based passive valving. Enhanced wettability of the PMMA surface can be used to securely hold the stationary liquid droplet under mechanical shock.

In this chapter, we present a "sample-to-answer" microfluidic reagent compact disc for field detection of *Pf* and *Pv*. The device uses a noncentrifugal method for solid-phase DNA extraction by actuating the DNA-carrying magnetic beads against the stationary reagent droplets. All reagents for streamlined sample process are preloaded and separated on the microfluidic reagent disc by teeth-shaped passive valves. The preloaded and ready-to-use microfluidic reagent disc contains four parallel testing units. It could be configured either as four identical tests to increase the testing throughput or as four species-specific tests to distinguish *Plasmodium* genus, *Pf and Pv* species. Each test unit automatically performs the parasite DNA binding, washing, elution, and immediate real-time isothermal amplification and fluorescence detection described in Chapter 14. This seamless integration from the sample to result on a single microfluidic reagent compact disc simplifies the complex

NATs process. The assay is performed with an automated device described in Chap. 14. The device could deliver sensitive (~0.5 parasites/μl) NAT results directly from a small volume of raw blood samples within 40 min for a material cost around $1/test.

2 Materials

2.1 Microfluidic Reagent Disc

1. Materials and supplies: Table 1.
2. CO_2 laser cutting machine (Epilog Helix 24 Laser System, USA).
3. Ultrasonic cleaning bath (CPX-952-218R, USA).
4. Cleaning reagents: Detergent, 2% (w/v) Sodium hypochlorite (NaOCl), and H_2O.
5. 0.030“ clear plexiglass acrylic sheet (ACRYCLR0.030PM26.5X43, ePlastics), 0.060” clear plexiglass acrylic sheet (ACRYCLR0.060FM24X48, ePlastics), acrylic adhesive Weld-On 4(IPS4-4OZ, ePlastics), PCR Plate Sealing Adhesive Film (MSB1001, Bio-Rad), water-oil repellent (UNIDYNE™ TG-5601, Daikin, Japan).
6. ChargeSwitch® Forensic DNA Purification Kits (CS11200, Invitrogen).

2.2 Loop-Mediated Isothermal Amplification Assay

1. LAMP master mix (25 μl): isothermal buffer (20 mM Tris–HCl, 10 mM $(NH_4)_2SO_4$, 50 mM KCl, 2 mM $MgSO_4$, 0.1% Tween 20, pH 8.8), PCR grade H_2O, $MgSO_4$ (7 mM), Betaine (0.4 M) $MnCl_2$ (0.75 mM), calcein (25 μM), deoxyribonucleotide triphosphates (dNTPs, 1.4 mM), *Bst* 2.0 DNA polymerase, DNA template, and primer sets (0.2 mM F3 and B3c, 1.6 mM FIP and BIP, and 0.8 mM LF and LB) (*see* Table 2).
2. Primer sets for the genus-, *Pf*-, and *Pv*-specific LAMP amplification are listed in Table 3.

3 Methods

The microfluidics assay presented in this chapter is performed with an automated device described in Chap. 14.

3.1 Microfluidic Reagent Compact Disc Fabrication

1. The microfluidic reagent compact disc has a diameter of 9.6 cm and a thickness of 3.2 mm. The top, spacer, and bottom polymethyl methacrylate (PMMA), known as acrylic, layers are designed using AutoCAD and patterned by a CO_2 laser cutting machine (Laser power: 75 W).
2. Figure 1a shows the separate image of each laser-patterned layer before assembly. All reagent loading inlets are patterned

Table 1
Microfluidic reagent disc cost. Bill of materials for the analyzer. (Reproduced from Biosensors and Bioelectronics 2018 with permission from Elsevier [50])

Reagents	Vendor	Function	Stock vol. (ml)	Unit cost ($)	Vol. (μl)/test	Ext. cost ($)/ test
Ultrapure PCR water	VWR	LAMP master mix	20	91.88	7.25	0.033
F3	IDT	LAMP master mix	1.4	9.22	0.25	0.002
B3	IDT	LAMP master mix	1.5	10.22	0.25	0.002
FIP	IDT	LAMP master mix	1.0	7.14	2.00	0.013
BIP	IDT	LAMP master mix	1.4	9.18	2.00	0.013
LF	IDT	LAMP master mix	1.7	11.86	1.00	0.007
LB	IDT	LAMP master mix	1.3	8.61	1.00	0.007
Calcein	Sigma-Aldrich	LAMP master mix	8000	133.00	0.63	0.000
$MnCl_2$	Sigma-Aldrich	LAMP master mix	100	62.60	1.88	0.001
Betaine	Sigma-Aldrich	LAMP master mix	1.5	24.25	2.00	0.032
dNTP mix	Thermo fisher	LAMP master mix	3.2	107.00	3.50	0.117
Bst polymerase	NEB	LAMP master mix	1	264.00	1.00	0.264
NEB isothermal buffer	NEB	LAMP master mix	6	24.00	2.5	0.010
$MgSO_4$	NEB	LAMP master mix	6	20.00	1.75	0.006
Lysis buffer	Invitrogen	Sample Prep.	800	142.00	1000.00	0.178
Binding buffer	Invitrogen	Sample Prep.	20	28.97	30.00	0.043
Wash buffer	Invitrogen	Sample Prep.	100	144.84	150.00	0.217
Proteinase K	Invitrogen	Sample Prep.	1	1.45	10.00	0.014
Magnetic beads	Invitrogen	Sample Prep.	2	2.90	10.00	0.014
Acrylic adhesive	ePlastics	Compact disc	118	9.69	1.5	0.041
1/32″ acrylic sheet	ePlastics	Compact disc	–	14.98	–	0.025
1/16″ acrylic sheet	ePlastics	Compact disc	–	17.72	–	0.030
					Total costTotal cost	**$ 1.07**

Table 2
Reagent setup of the LAMP master mix. (Reproduced from Lab on a Chip 2016 with permission from the Royal Society of Chemistry [50])

Component	Concentration	Volume (μl)
PCR grade water	1×	4.25
Primer sets	–	6.50
Isothermal buffer	1×	2.50
Betaine	0.4 M	2.00
$MgSO_4$	7.00 mM	1.75
Calcein	25.00 μM	0.63
$MnCl_2$	0.75 mM	1.88
dNTP mix	1.40 mM	3.50
Bst DNA polymerase	0.32 Unit/μl	1.00

on 0.03″ thick top layer. 0.06″ thick spacer with 0.03″ thick bottom layer provides chambers to hold all reagents such as binding, washing, and LAMP master mix (Figs. 1 and 2).

3. The patterned top, spacer, and bottom PMMA layers are initially washed with detergent to remove residues from laser cutting.
4. All three layers are aligned using the alignment hole and permanently laminated with adhesive solvent. Before applying the adhesive, we stack patterned layers and align them using alignment holes (Fig. 1b). The liquid adhesive solvent is applied by a syringe from the side of the disc. The small gap between PMMA layers induces capillary action and aids the adhesive solvent in flowing naturally over the area. Pressing the PMMA layers disturbs the capillary action; thus, it is not recommended. Although adhesive showed a good amount of bonding strength after 5 min, we normally cure more than 1 h at room temperature for better bonding.
5. The assembled disc is cleaned with 2% sodium hypochlorite (NaOCl) and distilled water in order to eliminate inhibitory substances, which could cause chemical interference (*see* **Note 1**).
6. The assembled disc has four testing units, and each unit contains three working chambers (Fig. 2): binding (220 μl), washing (150 μl), and reaction chambers (25 μl).
7. Each reagent chamber is isolated by a valve chamber (80 μl) to prevent the reagent mixing. The valving chambers are filled with FC-40 oil or air (Figs. 1 and 3). The FC-40 oil, which seals the LAMP reaction chamber, helped prevent master mix

Table 3
Primer sets for the genus-, *Pf*-, and *Pv*-specific LAMP amplification. (Reproduced from Biosensors and Bioelectronics 2018 with permission from Elsevier [50])

Species	Primer	Sequence (5′ → 3′)
Plasmodium genus	F3	TCGCTTCTAACGGTGAACT
	B3c	AATTGATAGTATCAGCTATCCATAG
	FIP (F1c–F2)	GGTGGAACACATTGTTTCATTTGATCTCATTCCAATGGAACC TTG
	BIP (B1–B2c)	GTTTGCTTCTAACATTCCACTTGCCCGTTTTGACCGGTCATT
	LF	CACTATACCTTACCAATCTATTTGAACTTG
	LB	TGGACGTAACCTCCAGGC
P. falciparum	F3	CTCCATGTCGTCTCATCGC
	B3c	AACATTTTTTAGTCCCATGCTAA
	FIP (F1c–F2)	ACCCAGTATATTGATATTGCGTGACAGCCTTGCAATAAATAA TATCTAGC
	BIP (B1–B2c)	AACTCCAGGCGTTAACCTGTAATGATCTTTACGTTAAGGGC
	LF	CGGTGTGTACAAGGCAACAA
	LB	GTTGAGATGGAAACAGCCGG
P. vivax	F3	GGTACTGGATGGACTTTATAT
	B3c	GGTAATGTTAATAATAGCATTACAG
	FIP (F1c–F2)	CCAGATACTAAAAGACCAACCCACCATTAAGTACATCACT
	BIP (B1–B2c)	GCTAGTATTATGTCTTCTTTCACTTAATATACCAAGTG TTAAACC
	LF	GATAACATCTACTGCAACAGG
	LB	CTACTGTAATGCATCTAAGATC

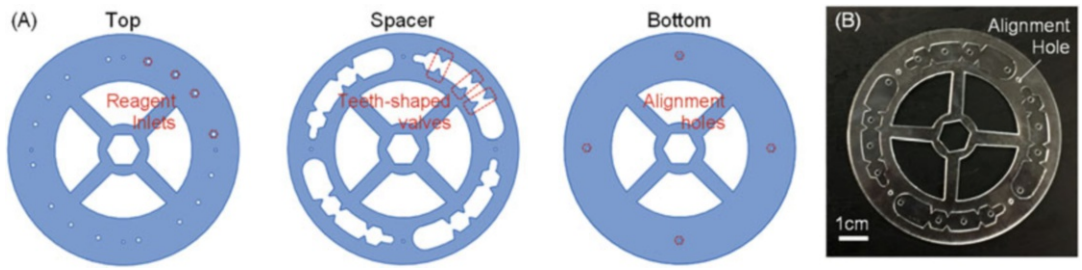

Fig. 1 (**a**) Schematics of the laser-patterned PMMA layers for microfluidic reagent disc fabrication. The top layer has inlets for reagent loading. The spacer layer has reagent chambers and valves (*see* Fig. 2b for the functionality of each chamber). (**b**) Photo image of the assembled disc

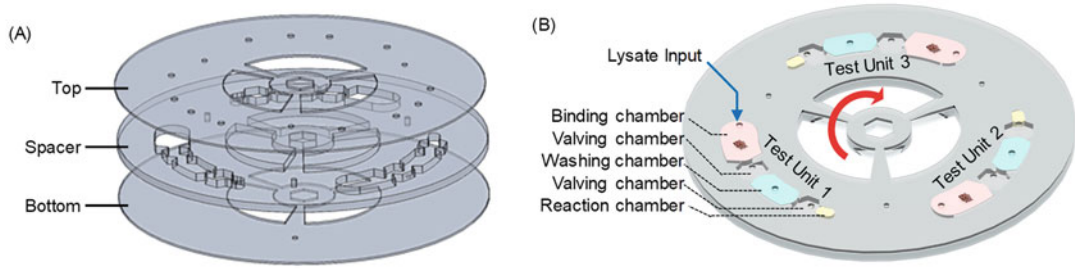

Fig. 2 Illustration of reagent compact disc and integrated sample preparation on the compact disc. (**a**) Exploded view of the reagent compact disc showing three-patterned PMMA layers. (**b**) Assembled view of the reagent compact disc showing three independent testing units. Each test unit consists of five chambers: a DNA binding chamber (binding buffer pH 5.0), a washing chamber (washing buffer pH 7.0), a LAMP reaction chamber (master mix, pH 8.8), and two valving chambers. All reagents are preloaded on the compact disc in a ready-to-use format. The lysate was prepared by collecting 20 μl malaria-infected blood into 1 ml of lysis buffer in a microcentrifuge tube. (Reproduced from Lab on a Chip 2016 with permission from the Royal Society of Chemistry [50])

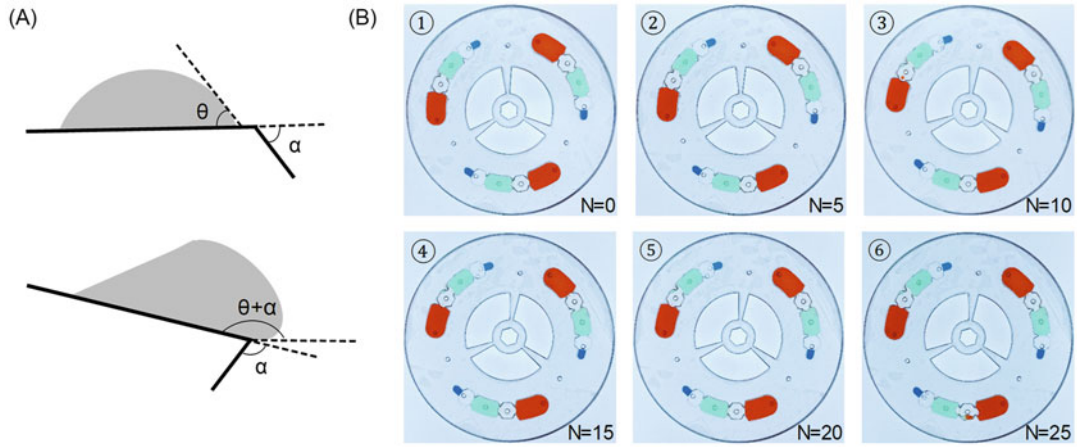

Fig. 3 Illustration of the pinning effect and photo images of the drop test results. (**a**) A droplet on a solid surface with a contact angle of θ, which will be increased up to $\theta + \alpha$ when moving toward a three-phase edge, where α is a bending angle [34]. This implies that larger α allows a higher activation barrier for the passive valve. (**b**) The drop test to evaluate the robustness of the teeth-shaped passive valves on the reagent compact disc under the harsh mechanical vibration (*N* denotes the number of drops). (Reproduced from Lab on a Chip 2016 with permission from the Royal Society of Chemistry [50])

evaporation during the thermal process. The air-filled valve is surface treated with water-oil repellent to create a barrier for the amphiphilic lysis buffer (*see* **Note 2** for surface treatment technique). Unlike other lab-on-a-chip devices, there is no liquid movement in the reagent compact disc. Instead, magnetic beads are moved from chamber to chamber by magnetic interaction and disc rotation. Therefore, active valving is not

necessary for the system. (The detailed description for the tooth-shaped active valve is available in Subheading 3.2).

8. All liquid phase reagents (beads, washing buffer, and LAMP master mix) and FC-40 oil are loaded into the designated chamber in the disc immediately before use (Fig. 2 and **Note 3**). The loading order is the master mix (25 μl, reaction chamber), FC-40 oil (80 μl, valving chamber), washing buffer (150 μl, washing chamber), binding buffer (30 μl, binding chamber), and magnetic beads (10 μl, binding chamber) (Fig. 2b). The reagents could also be preloaded into the disc and would last for at least 1 week if stored at 4 °C.
9. After the sample loading, the whole disc is sealed with pressure-sensitive adhesive (PSA) to avoid potential cross-contamination from the environment.

3.2 Robustness Under Mechanical Shock

1. Structural pinning effect [34, 35] and modified surface tension are the underlying principles that enable the teeth-shaped valves to hold the liquid in each chamber securely. The pinning effect refers to the fact that a sharp bending angle (α) of the teeth structure radically increases the liquid/vapor interface area and raises the activation energy, which prevents fluid from overcoming the barrier (Fig. 1—spacer layer and Fig. 3) [34]. The enhanced surface tension is another important aspect of our passive valve structure. The valve surface is treated with water-oil repellent to increase the activation barrier by introducing a higher surface tension [34], which also helps circumvent cross-contamination during sample preparation.
2. To demonstrate the robustness of the passive valve for preventing the reagents from mixing under the harsh mechanical vibration, we perform a drop test on the microfluidic compact disc. Three different colors of food dyes are preloaded into each reagent chamber for visualization of any liquid movement. Each reagent-loading hole is sealed with pressure-sensitive adhesive (PSA) to prevent leakage. The disc is dropped from a height of 20 cm along a guiding rod toward a rigid surface for 25 times. The disc is inspected every five drops with naked eyes to confirm the functionality of the valve. The result showed that the teeth-shaped valve endured 25 consecutive drops without reagents mixing (Fig. 3).

3.3 The Workflow of Malaria Blood Testing

The reagent compact disc is equipped with a real-time fluorescence detector (discussed in Chapter 1) to perform a streamlined process. The workflow of the device consists of four steps (Fig. 4).

1. The 20 μl of finger-prick blood is collected using a capillary tube and lysed in the collection tube filled with 1000 μl of lysis buffer.

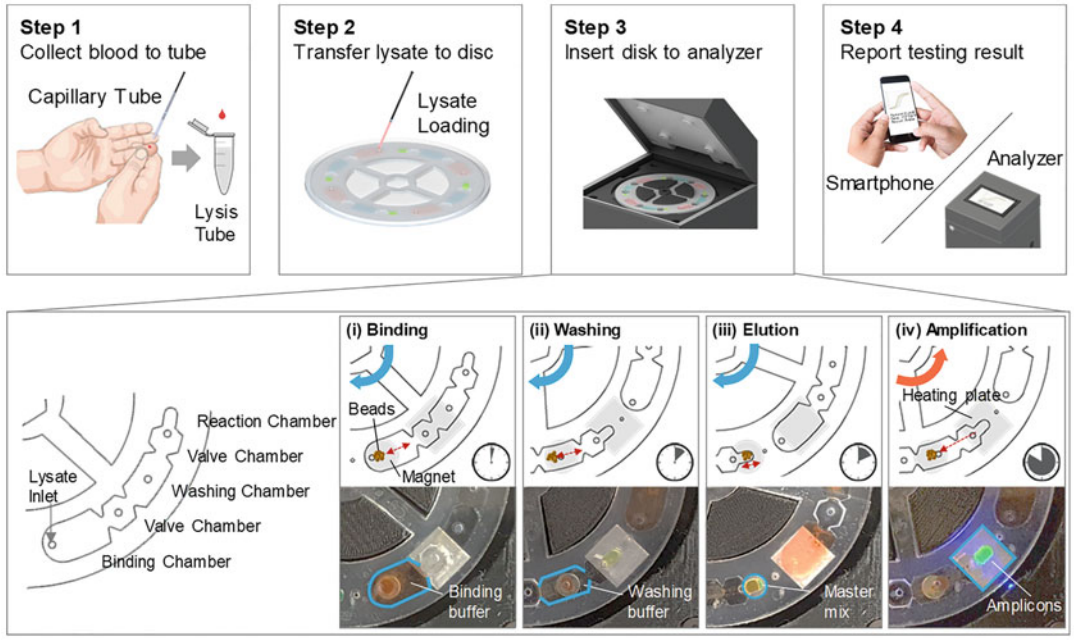

Fig. 4 The workflow of the device. In step 1, whole blood is collected into the lysis buffer by the capillary tube. In step 2, the lysate is loaded into the binding chamber of the four testing units. In step 3, the disc is sealed and inserted into the analyzer, which then performs automated sample preparation and amplification. This automated process consists of four steps: binding (3 min), washing (4 min), elution (3 min), and amplification (40 min). During the amplification process, the real-time fluorescence signal from each testing unit was recorded and analyzed. Finally, in step 4, the testing results are reported. (Reproduced from Biosensors and Bioelectronics 2018 with permission from Elsevier [51])

2. 180 μl of blood lysate is transferred into each binding chamber of the testing units on the reagent compact disc.
3. After loading the sample, the disc is sealed with PSA tape and inserted into the mobile analyzer for a streamlined nucleic acid sample preparation and amplification process (enlarged view of **step 3** in Fig. 4).
4. During the amplification, the fluorescence intensity data are recorded on a nonvolatile memory card and displayed on the LCD screen in real time. Users also have an option to receive the results using a smartphone.

3.4 Streamlined Sample Preparation

In contrast to the conventional lab-on-a-disc devices that rely on energy-hungry centrifugal forces [36–39], a noncentrifugal and energy-efficient magnetic interaction method is used. More specifically, the pH charge switchable magnetic beads are directed from chamber to chamber by rotating the disc against a stationary magnet underneath of the disc. The process for each sample consists of the following three steps: binding, washing, and elution (**step 3** of Fig. 4).

1. The negatively charged parasite DNAs first bind to the pH-sensitive charge-switchable magnetic beads at pH 5.0. During the binding process (~3 min), the reagent compact disc is rotated back and forth slowly to ensure thorough mixing of the beads and the lysate. More specifically, the initial disc position is where the binding chamber inlet is aligned with the permanent magnet underneath the disc (*see* **step 3** of Fig. 4). The disc rotates by the servo control until the magnet locates underneath the entrance of the air-filled valve chamber. Due to the magnetic interaction, the magnetic beads are actuated toward the valve entrance, where the magnet is positioned. Then, we rotate back the disc to the initial position and repeat the process to capture the maximum number of DNA-binding magnetic beads. Once this process is completed, the DNA-binding magnetic beads are transferred to the washing chamber by magnetic actuation.
2. The DNA washing process lasts for about 4 min, and the magnetic beads with purified DNAs are further transferred to the reaction chamber (LAMP master mix).
3. The LAMP master mix has a pH of 8.8, which switches the surface charge of the magnetic beads toward negative. The negatively charged DNAs are therefore repelled off from the magnetic beads and eluted into the master mix.
4. The residual magnetic beads are removed from the reaction chamber before initiating the LAMP reaction. The entire sample preparation is multiplexed for four samples and could be finished in less than 10 min with minimal user intervention.

3.5 Primer Validation

1. To validate the LAMP primer sets for specifically detecting *Pf*, *Pv*, and pan-Plasmodium, we perform a cross-reactivity test using extracted *Pf* and *Pv* genomic DNA on a benchtop real-time PCR instrument (Bio-Rad CFX96). Each analysis is performed in triplicate.
2. As shown in Fig. 5a, *Pf*- and *Pv*- specific assays can pick up the corresponding genomic sample specifically without cross-reactivity. In contrast, the pan-Plasmodium assays can pick up any *Plasmodium* species (*Pf* and *Pv*). No amplification is observed with the negative control (PCR grade water).
3. We perform gel electrophoresis in 2% agarose gel to further evaluate each amplicon (Fig. 5b). A clear ladder-like pattern with multiple bands of different molecular sizes is observed due to the stem-loop DNA structures with several inverted repeats within LAMP amplicons [40]. The length of the bands show confirmative agreement with the length of the target sequence (213-, 127-, and 220-bp bands are expected from *Pf*, *Pv*, and pan-Plasmodium products, respectively) [41, 42].

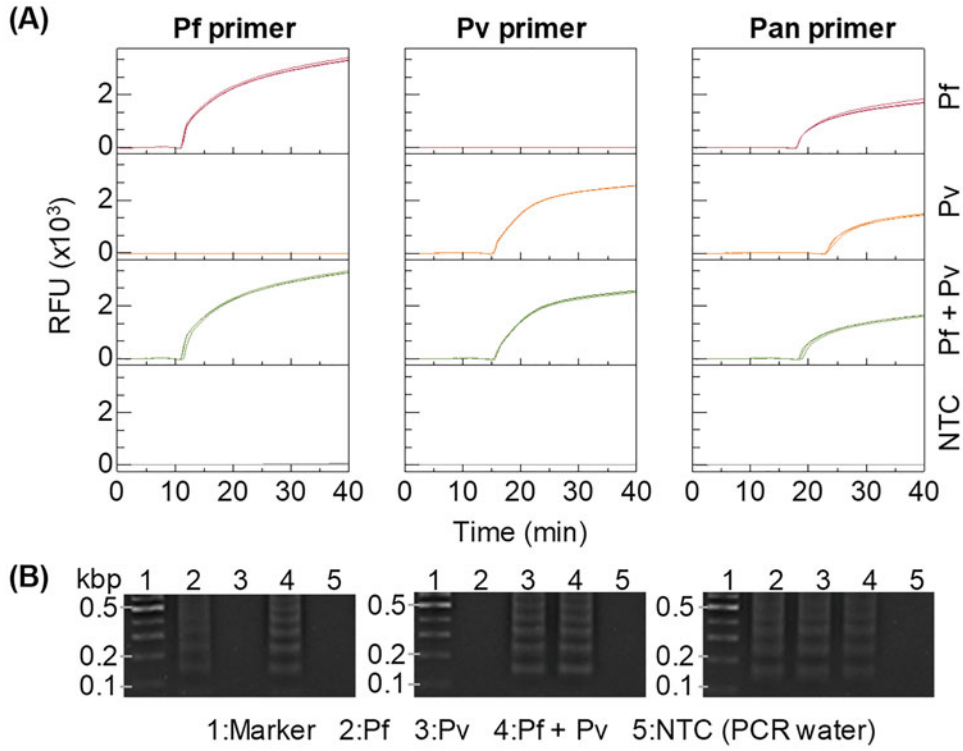

Fig. 5 Validation of the species- and genus-specific LAMP assays using laboratory purified *Pf* and *Pv* genomic DNA. (**a**) Amplification curves obtained from real-time PCR. PCR grade water was used as a no template control (NTC). (**b**) Gel electrophoresis image (2% agarose gel). Ladder-like bands in the gel image confirm the amplicons from species- and genus-specific LAMP reactions. (Reproduced from Biosensors and Bioelectronics 2018 with permission from Elsevier [51])

3.6 Sensitivity Test

1. To evaluate the analytical sensitivity of our device in the real-world settings, we ten-fold diluted the *Pf*-infected whole blood with healthy blood to create mock samples with 10-6% to 1% parasitemia. The parasite DNA samples are automatically prepared on the compact disc. Each parasitemia sample is performed in triplicate, together with negative control on a single disc (four reactions per run).
2. As shown in Fig. 6a, a whole blood sample with parasitemia higher than 10^{-5}% could be identified. Since parasitemia is the ratio of the parasitized RBCs to the total RBCs, 10^{-5}% parasitemia would correspond to 0.5 parasites/μl (normal RBC count is ~5×10^6 cells/μl [3]). Although a rigorous report of the limit of detection (i.e., analytical sensitivity) requires a statistical comparison with the analytical blank and should be expressed as a probability with confidence intervals [43], a quick eyeball of the data shown in Fig. 6a suggests the whole blood sensitivity is around 0.5 parasites/μl. The WHO estimates that analytical sensitivity needs to be lower than

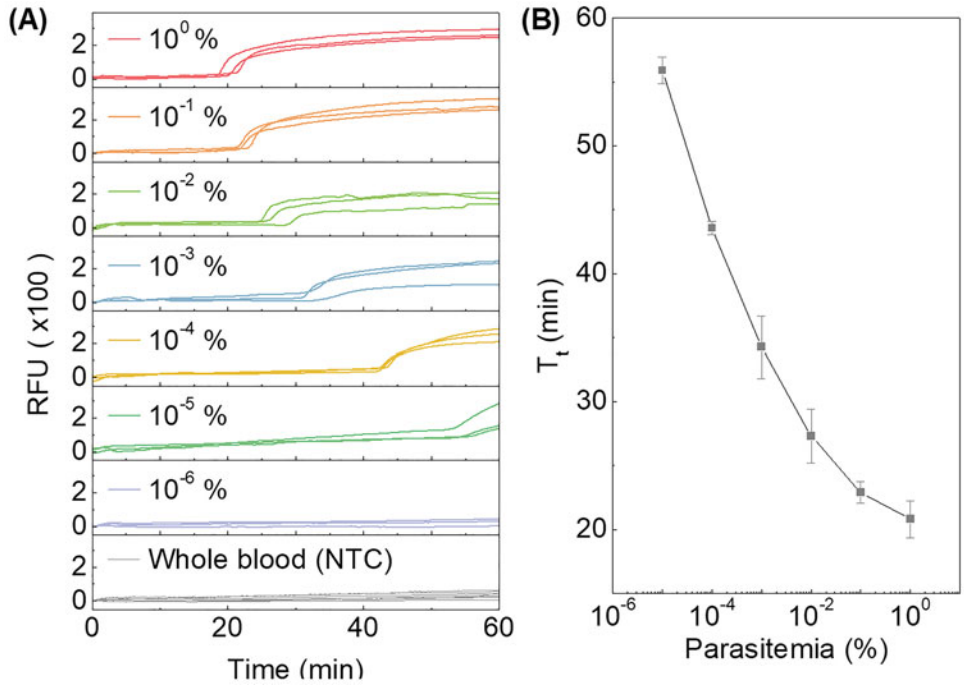

Fig. 6 Sensitivity test with *Pf*-infected whole blood sample (**a**) Amplification curves for tenfold serially diluted *Pf*-infected whole blood samples. Healthy human blood was used as an NTC. (**b**) The resulting calibration curve for the whole blood sample. Standard deviation values are from triplicates. (Reproduced from Biosensors and Bioelectronics 2018 with permission from Elsevier [51])

2 parasites/μl for identifying low-level infection in a preelimination setting [44]. This sensitivity achieved in our device is comparable to other NAT methods (1–5 parasites/μl) [25] and suitable for detecting low-level asymptomatic carriers [2, 45–47]. No amplification is observed for the healthy whole blood sample, which suggests the background human genomic DNA has negligible interferences.

3. The amplification threshold time (T_t) is extracted for each parasitemia, and the results are shown in Fig. 6b. The inversely proportional relationship between T_t and parasitemia confirmed that the quantitative ability is still valid with whole blood samples. It is interesting to note that the calibration curve shown in Fig. 6b is not exactly linear, which is likely because the DNA extraction efficiency is nonlinear for different cell numbers [48].

3.7 Specificity Test

1. To evaluate the specificity of the device, we prepare whole blood samples spiked randomly with *Pf* and *Pv*. Those sample's species information is recorded but blinded to the tester. The reagent compact disc is configured as species-specific tests, as shown in Fig. 7a. Each test disc incorporates an internal

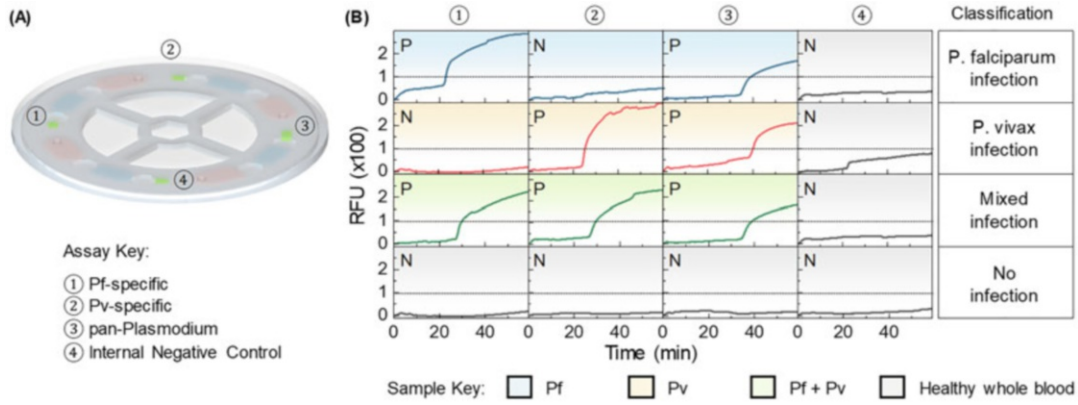

Fig. 7 Species- and genus-specific tests using spiked whole blood samples. (**a**) The reagent compact disc was configured as species-specific tests. The testing unit 1 and 2 contains *Pf*- and *Pv*- specific primer sets, respectively. The testing unit 3 has a genus-specific primer set. Testing unit 4 is for internal negative control. (**b**) The result from a representative set of samples (i.e., *Pf*, *Pv*, mixed, and healthy). A threshold of 100 RFU (dashed line) is experimentally determined for positive and negative differentiation. The species information for a particular infected whole blood sample can be derived from four qualitative results on the single microfluidic disc (each row). (Reproduced from Biosensors and Bioelectronics 2018 with permission from Elsevier [51])

negative control unit to monitor the test quality. A threshold of 100 RFU is experimentally determined to differentiate positive and negative results.

2. Figure 7b shows the result from a representative set of samples (i.e., *Pf*, *Pv*, mixed, and healthy). The species information for a particular infected whole blood sample can be derived from four qualitative results on the single microfluidic disc. For example, the *Pf*-infected sample (first row of Fig. 7b) can be identified by the *Pf*-specific assay as well as the genus-specific assay. In contrast, the mixed infection sample can be detected when *Pf*-, *Pv*-, and genus-specific assays all show positive. Since *Pf* and *Pv* are the two most prevalent species that pose the greatest threat to the human, identification of these major malaria parasite species in the field could provide the malaria transmission profile to the healthcare workers and enable the effective malaria eradication strategy [25].

3.8 Test Cost Analysis

1. The disposable reagent compact disc (including the sample preparation and the amplification reagents) costs ~$1.07 per each test (Table 1). Note that this cost analysis is only to provide a ballpark figure to the interested researchers to replicate the system.

4 Notes

1. Detergent and distilled water are not sufficient to eliminate the amplification inhibitors in microfluidic reagent compact disc, often cause false-negative results. Sodium hypochlorite (NaOCl) is a strong oxidizing agent, an effective decontaminating reagent for various contaminants such as organic/inorganic chemicals, proteins, enzymes, and nucleic acids [49]. To remove the potential contaminants, all functional chambers are filled with a 2% NaOCl solution for 30 min, then thoroughly washed with distilled water. The washed chambers are blow-dried with compressed air.
2. To treat the PMMA surface, the valving chamber is first filled with liquid phase water–oil repellent for 2 min, then removed using a pipette. The repellent wetted PMMA surface is dried at 150 °C for 2 min. The treated surface has a lower interaction with liquids than the internal interaction within the liquid, thus repels the water-based amphiphilic lysis buffer.
3. While loading the liquid phase reagent, air bubbles can be easily trapped in the chamber. Air bubbles possibly disrupt the magnetic bead movements in the reagent chamber. If air bubbles are trapped in the reaction chamber, they interfere with the optical signal since the bubbles move during the thermal process. Slightly lifting the binding chamber side of the testing unit during the loading process is helpful in avoiding trapping of air bubbles.

Acknowledgments

This work was supported by grants National Science Foundation under Grant No. 1710831, 1912410, and 1902503. We express our gratitude to Dr. Liwang Cui, Dr. Jun Miao, and Xiaolian Li for providing malaria samples. The following reagent is obtained through BEI Resources Repository, NIAID, NIH: *Plasmodium vivax*, Strain Chesson, MRA-383, and strain Achiote, MRA-369, contributed by W. E. Collins. W.G. acknowledges the support from Penn State Startup Fund.

References

1. Slater HC, Ross A, Ouedraogo AL et al (2015) Assessing the impact of next-generation rapid diagnostic tests on *Plasmodium falciparum* malaria elimination strategies. Nature 528 (7580):S94–S101
2. Wongsrichanalai C, Barcus MJ, Muth S et al (2007) A review of malaria diagnostic tools: microscopy and rapid diagnostic test (RDT). Am J Trop Med Hyg 77(6):119–127

3. Moody A (2002) Rapid diagnostic tests for malaria parasites. Clin Microbiol Rev 15 (1):66–78
4. Snounou G, Viriyakosol S, Zhu XP et al (1993) High-sensitivity of detection of human malaria parasites by the use of nested polymerase chain-reaction. Mol Biochem Parasit 61(2):315–320
5. Han ET, Watanabe R, Sattabongkot J et al (2007) Detection of four plasmodium species by genus- and species-specific loop-mediated isothermal amplification for clinical diagnosis. J Clin Microbiol 45(8):2521–2528
6. Reddy V, Ravi V, Desai A et al (2012) Utility of IgM ELISA, TaqMan real-time PCR, reverse transcription PCR, and RT-LAMP assay for the diagnosis of chikungunya fever. J Med Virol 84 (11):1771–1778
7. Britton S, Cheng Q, McCarthy JS (2016) Novel molecular diagnostic tools for malaria elimination: a review of options from the point of view of high-throughput and applicability in resource limited settings. Malar J 15 (1):88
8. Oriero EC, van Geertruyden JP, Nwakanma DC et al (2015) Novel techniques and future directions in molecular diagnosis of malaria in resource-limited settings. Expert Rev Mol Diagn 15(11):1419–1426
9. Goyal K, Kaur H, Sehgal A et al (2015) RealAmp loop-mediated isothermal amplification as a point-of-care test for diagnosis of malaria: neither too close nor too far. J Infect Dis 211 (10):1686
10. Morris U, Khamis M, Aydin-Schmidt B et al (2015) Field deployment of loop-mediated isothermal amplification for centralized mass-screening of asymptomatic malaria in Zanzibar: a pre-elimination setting. Malar J 14:205
11. Hsiang MS, Greenhouse B, Rosenthal PJ (2014) Point of care testing for malaria using LAMP, loop mediated isothermal amplification. J Infect Dis 210(8):1167–1169
12. Patel JC, Lucchi NW, Srivastava P et al (2014) Field evaluation of a real-time fluorescence loop-mediated isothermal amplification assay, RealAmp, for the diagnosis of malaria in Thailand and India. J Infect Dis 210 (8):1180–1187
13. Han ET (2013) Loop-mediated isothermal amplification test for the molecular diagnosis of malaria. Expert Rev Mol Diagn 13 (2):205–218
14. Singh R, Savargaonkar D, Bhatt R et al (2013) Rapid detection of Plasmodium vivax in saliva and blood using loop mediated isothermal amplification (LAMP) assay. J Infect 67 (3):245–247
15. Surabattula R, Vejandla MP, Mallepaddi PC et al (2013) Simple, rapid, inexpensive platform for the diagnosis of malaria by loop mediated isothermal amplification (LAMP). Exp Parasitol 134(3):333–340
16. Sirichaisinthop J, Buates S, Watanabe R et al (2011) Evaluation of loop-mediated isothermal amplification (LAMP) for malaria diagnosis in a field setting. Am J Trop Med Hyg 85 (4):594–596
17. Sattabongkot J, Tsuboi T, Han ET et al (2014) Loop-mediated isothermal amplification assay for rapid diagnosis of malaria infections in an area of endemicity in Thailand. J Clin Microbiol 52(5):1471–1477
18. Kersting S, Rausch V, Bier FF et al (2014) Rapid detection of Plasmodium falciparum with isothermal recombinase polymerase amplification and lateral flow analysis. Malar J 13:99
19. Cordray MS, Richards-Kortum RR (2015) A paper and plastic device for the combined isothermal amplification and lateral flow detection of plasmodium DNA. Malar J 14:472
20. Li Y, Kumar N, Gopalakrishnan A et al (2013) Detection and species identification of malaria parasites by isothermal, tHDA amplification directly from human blood without sample preparation. J Mol Diagn 15(5):634–641
21. Liu Q, Nam J, Kim S et al (2016) Two-stage sample-to-answer system based on nucleic acid amplification approach for detection of malaria parasites. Biosens Bioelectron 82:1–8
22. Xu G, Nolder D, Reboud J et al (2016) Paper-origami-based multiplexed malaria diagnostics from whole blood. Angew Chem 55 (49):15250–15253
23. Lucchi NW, Gaye M, Diallo MA et al (2016) Evaluation of the Illumigene malaria LAMP: a robust molecular diagnostic tool for malaria parasites. Sci Rep 6:36808. https://doi.org/10.1038/srep36808
24. Dineva MA, MahiLum-Tapay L, Lee H (2007) Sample preparation: a challenge in the development of point-of-care nucleic acid-based assays for resource-limited settings. Analyst 132 (12):1193–1199
25. Kolluri N, Klapperich CM, Cabodi M (2018) Towards lab-on-a-chip diagnostics for malaria elimination. Lab Chip 18:75–94
26. Sema M, Alemu A, Bayih AG et al (2015) Evaluation of non-instrumented nucleic acid amplification by loop-mediated isothermal amplification (NINA-LAMP) for the diagnosis of malaria in Northwest Ethiopia. Malar J 14:44. https://doi.org/10.1186/s12936-12015-10559-12939

27. Reboud J, Xu G, Garrett A et al (2019) Paper-based microfluidics for DNA diagnostics of malaria in low resource underserved rural communities. Proc Natl Acad Sci U S A 116 (11):4834–4842
28. Phillips EA, Moehling TJ, Ejendal KFK et al (2019) Microfluidic rapid and autonomous analytical device (microRAAD) to detect HIV from whole blood samples. Lab Chip 19 (20):3375–3386
29. Stumpf F, Schwemmer F, Hutzenlaub T et al (2016) LabDisk with complete reagent prestorage for sample-to-answer nucleic acid based detection of respiratory pathogens verified with influenza a H3N2 virus. Lab Chip 16 (1):199–207
30. Gorkin R, Park J, Siegrist J et al (2010) Centrifugal microfluidics for biomedical applications. Lab Chip 10(14):1758–1773
31. Sun Y, Quyen TL, Hung TQ et al (2015) A lab-on-a-chip system with integrated sample preparation and loop-mediated isothermal amplification for rapid and quantitative detection of salmonella spp. in food samples. Lab Chip 15(8):1898–1904
32. Chiu DT, deMello AJ, Di Carlo D et al (2017) Small but perfectly formed? Successes, challenges, and opportunities for microfluidics in the chemical and biological sciences. Chem 2 (2):201–223
33. Wang Z, Zheng H, Lim C et al (2009) Polymer hydrophilicity and hydrophobicity induced by femtosecond laser direct irradiation. Appl Phys Lett 95(11):111110
34. Gao LC, McCarthy TJ (2006) Contact angle hysteresis explained. Langmuir 22 (14):6234–6237
35. Oner D, McCarthy TJ (2000) Ultrahydrophobic surfaces. Effects of topography length scales on wettability. Langmuir 16(20):7777–7782
36. Madou M, Zoval J, Jia GY et al (2006) Lab on a CD. Annu Rev Biomed Eng 8:601–628
37. Kim TH, Park J, Kim CJ et al (2014) Fully integrated lab-on-a-disc for nucleic acid analysis of food-borne pathogens. Anal Chem 86 (8):3841–3848
38. Nolte DD (2009) Invited review article: review of centrifugal microfluidic and bio-optical disks. Rev Sci Instrum 80(10):101101
39. Kong LX, Perebikovsky A, Moebius J et al (2016) Lab-on-a-CD: a fully integrated molecular diagnostic system. J Lab Autom 21 (3):323–355
40. Notomi T, Okayama H, Masubuchi H et al (2000) Loop-mediated isothermal amplification of DNA. Nucleic Acids Res 28(12):E63
41. Polley SD, Mori Y, Watson J et al (2010) Mitochondrial DNA targets increase sensitivity of malaria detection using loop-mediated isothermal amplification. J Clin Microbiol 48 (8):2866–2871
42. Britton S, Cheng Q, Grigg MJ et al (2016) Sensitive detection of Plasmodium vivax using a high-throughput, Colourimetric loop mediated isothermal amplification (HtLAMP) platform: a potential novel tool for malaria elimination. PLoS Negl Trop Dis 10(2): e0004443
43. Long GL, Winefordner JD (1983) Limit of detection. A closer look at the IUPAC definition. Anal Chem 55(7):712A–724A
44. WHO (2017) World Malaria Report 2017. 1-196
45. Vallejo AF, Martinez NL, Gonzalez IJ et al (2015) Evaluation of the loop mediated isothermal DNA amplification (LAMP) kit for malaria diagnosis in P. vivax endemic settings of Colombia. PLoS Negl Trop Dis 9(1):e3453
46. Modak SS, Barber CA, Geva E et al (2016) Rapid point-of-care isothermal amplification assay for the detection of malaria without nucleic acid purification. Infect Dis 9:1–9
47. Hopkins H, Gonzalez IJ, Polley SD et al (2013) Highly sensitive detection of malaria parasitemia in a malaria-endemic setting: performance of a new loop-mediated isothermal amplification kit in a remote clinic in Uganda. J Infect Dis 208(4):645–652
48. Katevatis C, Fan A, Klapperich CM (2017) Low concentration DNA extraction and recovery using a silica solid phase. PLoS One 12(5): e0176848
49. Wilson IG (1997) Inhibition and facilitation of nucleic acid amplification. Appl Environ Microb 63(10):3741–3751
50. Choi G, Song D, Shrestha S et al (2016) A field-deployable mobile molecular diagnostic system for malaria at the point of need. Lab Chip 16(22):4341–4349
51. Choi G, Prince T, Miao J et al (2018) Sample-to-answer palm-sized nucleic acid testing device towards low-cost malaria mass screening. Biosens Bioelectron 115:83–90